Solid-State Electronics 63 (2011) 130–136

Contents lists available at ScienceDirect

Solid-State Electronics

journal homepage: www.elsevier.com/locate/sse

A straightforward method to extract the shunt resistance of photovoltaic cells from current–voltage characteristics of mounted arrays

Vincenzo d'Alessandro *, Pierluigi Guerriero, Santolo Daliento, Matteo Gargiulo

Department of Biomedical, Electronics, and Telecommunications Engineering, University of Naples Federico II, via Claudio 21, 80125 Naples, Italy

ARTICLE INFO

Article history:
Received 30 January 2011
Accepted 18 May 2011
Available online 12 June 2011

The review of this paper was arranged by Prof. S. Cristoloveanu

Keywords:
Bypass diode
Five-parameter model
I–V characteristic
One-diode equivalent circuit
Photovoltaic (PV) cells
PV string
Series resistance
Shunt resistance

ABSTRACT

A straightforward non-invasive method is proposed to accurately evaluate the shunt resistance of an elementary cell of a photovoltaic module connected in an installed string without requiring prior knowledge of the parameters of the intrinsic diodes. The approach relies on the measurement of the current–voltage characteristic of the whole string after intentionally shading the selected cell. Calibrated PSPICE simulations are employed to illustrate the method and test its reliability. As a case study, the shunt resistances of several cells belonging to a series array of 10 commercial panels are determined.

1. Introduction

The shunt resistance R_{sh} is a lumped component usually included in the equivalent circuits of a photovoltaic (PV) cell to describe the existence of alternative paths for the current flow through the inherent diode or along the cell edges. This parasitic parameter can be reviewed as an indicator of the cell quality, since the shunt paths are due to manufacturing defects as e.g., lattice imperfections or impurities in/near the depletion region [1], and penetration of the front contacts through the P–N junction [2,3], which can be non-uniformly distributed over the cell area [2–4]. If the value of R_{sh} is low, i.e., the shunt paths exhibit a high conductance, large leakage currents are undesirably derived. This in turn entails a performance degradation of the PV field due to the reduction in the power produced, especially at low irradiation levels (e.g., during cloudy days and/or far from noon) [5–7]. The shunt currents might also affect the open-circuit voltage V_{oc} and short-circuit current I_{sc} of cells characterized by intolerably low quality (i.e., with $R_{sh} < 0.5\ \Omega$). Moreover, low-R_{sh} cells are particularly susceptible to *hot-spot* formation when shaded [7].

It is commonly recognized that an accurate assessment of the shunt resistance (not usually provided by the manufacturer) and of the other key cell parameters is of utmost importance for the design optimization of PV systems due to the increased reliability of the models implemented in simulation tools, as well as for quality control and performance estimation. Several extraction approaches have indeed been developed and proposed in the literature, which are based on the measurement of current–voltage (*I–V*) characteristics of the individual cell under (different levels of) illumination or in the dark. In particular, R_{sh} is conventionally determined from the slope of the *I–V* curve where the behavior of the cell is assumed to be dominated by the shunt loss, namely, (i) at low forward voltages [8,9], (ii) in the short-circuit current point (either *directly* [10–16] or through the simultaneous solution of a system of non-linear equations derived under illumination [17–19] or in the dark [20]), and (iii) in the reverse region [13,21–24]. However, practical difficulties are to be faced when performing this extraction, since soft-breakdown phenomena often arising at low reverse voltages in silicon cells [6,25,26] may significantly reduce the voltage span within which the slope is solely determined by the shunt resistance, thus affecting the accuracy of the results. In other works, R_{sh} is evaluated concurrently with all other cell parameters on the basis of a single experimental *I–V* characteristic by adopting analytical relations describing the most relevant points of the curve [27], fitting procedures relying on the least-squares method [28,29], and even genetic algorithms [30]. Lastly, a direct technique, which makes use of the V_{oc} and I_{sc} values measured under very low irradiance conditions, was proposed in [31] and successfully compared to a traditional slope-based method in [8].

* Corresponding author. Tel.: +39 081 7683509; fax: +39 081 7685925.
E-mail address: vindales@unina.it (V. d'Alessandro).

0038-1101/$ - see front matter © 2011 Elsevier Ltd. All rights reserved.
doi:10.1016/j.sse.2011.05.018

An important issue concerns the measurement of the shunt resistance of individual cells embedded in a commercial module, which can be in principle carried out only after a critical cell de-encapsulation, or using a sophisticated two-terminal procedure that relies on the simultaneous application of a DC voltage source, an AC signal generator, and an operational amplifier connected to a phase-sensitive lock-in amplifier [5]. As an alternative, one could perform a gross (i.e., low-granularity) quality testing by determining the R_{sh} corresponding to the *whole* panel. However, this approach is particularly prone to errors due to the enhanced flattening of the *I–V* curve, combined with the unavoidable data noise and the limited current resolution of available measurement systems; besides, it does not allow the identification of an uneven cell quality distribution within the module, or the detection of a cell failure.

In this work, we propose a simple non-intrusive technique to accurately quantify the shunt resistance of a selected PV cell belonging to a module connected in an installed string. The method relies on the measurement of the *I–V* curve of the whole string by keeping the cell under ideally dark conditions. An extensive analysis supported by the widespread simulation tool PSPICE [32] is performed, which proves that the method provides a fairly good accuracy without the need of a preliminary assessment of the ideality factor of the inherent diodes, even though the array includes a large number of series-connected cells. The approach is applied to a string comprising 10 commercial silicon panels with the aim to determine the cell quality distribution.

2. Experimental material and simulation approach

The experimental investigation was conducted on an array composed by 10 encapsulated mono-crystalline silicon 50 Wp modules, each partitioned into two sub-panels provided with a bypass diode (located in the *junction box* mounted on the rear) and comprising 20 elementary cells (with area equal to 68 cm^2) connected in series. As shown in Fig. 1, the string was mounted on the rooftop of the department for experimental purposes. The PV panels were individually characterized through a self-powered monitoring circuit recently developed *in house* for diagnostic services [33]: the open-circuit voltage V_{oc} of the individual modules was found to range between 20 and 25 V, while the short-circuit current I_{sc} was detected to span from 2 (winter) to 3 A (summer) around solar noon. A custom version of the H&H ZS3060 electronic DC load [34] rated for 3 kW and 800 V was employed to measure the *I–V* curves of the overall string.

The popular tool PSPICE – sometimes successfully applied to the analysis of PV cells/modules [5,35] – was adopted to explain the features and verify the accuracy of the proposed extraction method. The elementary cell was described through the equivalent lumped electrical circuit (often referred to as five-parameter single-diode model) represented in Fig. 2, which includes: a current source of photogenerated current I_{ph} (also denoted as photocurrent), an ideal (i.e., resistance-free) diode accounting for the dark *I–V* characteristic – fully defined by the reverse saturation current I_0 and the ideality factor n – and the parasitic series and shunt resistances, denoted with R_s and R_{sh}, respectively. This popular model, based on the so-called "superposition principle" [36], accurately describes the behavior of most PV cells under standard (i.e., non-stressed) operating conditions.

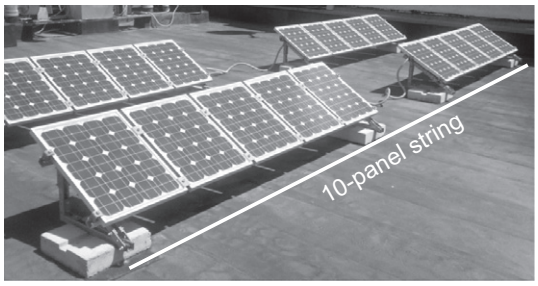

Fig. 1. Pair of 10-panel strings installed on the rooftop of the department. Each panel is partitioned into two 20-cell sub-panels equipped with a bypass diode located in the *junction box* mounted on the rear; the string includes 400 elementary cells.

3. The extraction method

The method is based on a straightforward experimental procedure, which requires that the PV string is fully exposed to sunshine, and can be described as follows.

The total series resistance of the string, denoted as $R_{s,string}$, can be expressed as:

$$R_{s,string} = \sum_{i=1}^{N}\sum_{j=1}^{M} R_{s,ij} + R_{bus} + R_{cab} \tag{1}$$

where N is the number of panels connected in series, M is the number of cells belonging to a panel, $R_{s,ij}$ is the series resistance associated to the j-th cell of the i-th panel, R_{bus} is the aggregate resistance of the bus bars, and R_{cab} is the resistance of the cables that ensure the connection to the measurement system. In order to determine $R_{s,string}$, we extended widely accepted approaches conceived to extract the series resistance of an individual cell, namely, the *method of the slope at the V_{oc} point* [10–12,14,16,17,37] yielding:

$$\begin{aligned} R_{s,string} &= -\left.\frac{dV_{string}}{dI_{string}}\right|_{V_{string}=V_{oc}} - N\cdot M\cdot\frac{n\cdot V_T}{I_{ph}+I_0} \\ &\approx -\left.\frac{dV_{string}}{dI_{string}}\right|_{V_{string}=V_{oc}} - N\cdot M\cdot\frac{n\cdot V_T}{I_{sc}} \end{aligned} \tag{2}$$

where $V_T = kT/q$ is the thermal voltage, T being the temperature of the modules, and the *area method* [38] leading to:

$$R_{s,string} = 2\cdot\left(\frac{V_{oc}}{I_{sc}} - \frac{P_A}{I_{sc}^2} - N\cdot M\cdot\frac{n\cdot V_T}{I_{sc}}\right) \tag{3}$$

where P_A is the area under the $I_{string} - V_{string}$ curve in the voltage range from 0 to V_{oc}.

As a first step, parameters I_{sc}, $\left.\frac{dV_{string}}{dI_{string}}\right|_{V_{string}=V_{oc}}$, V_{oc}, and P_A included in Eq. (2) and Eq. (3) are to be extracted from an experimental $I_{string} - V_{string}$ characteristic measured while the string is under full irradiation.

Afterward, a selected cell of the string is intentionally kept under ideally dark conditions (as shown in Fig. 3) and the $I_{string} - V_{string}$ characteristic is measured. A PSPICE simulation of a 2-panel string was performed to illustrate the behavior of the key electrical signals against string voltage; in particular, each panel is composed by 40 cells uniformly sharing $R_{sh} = 30\ \Omega$. For low V_{string} values, the voltage drop across the 20-cell sub-panel includ-

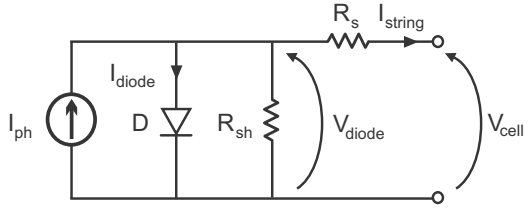

Fig. 2. Equivalent 5-parameter one-diode electrical circuit of a PV cell.

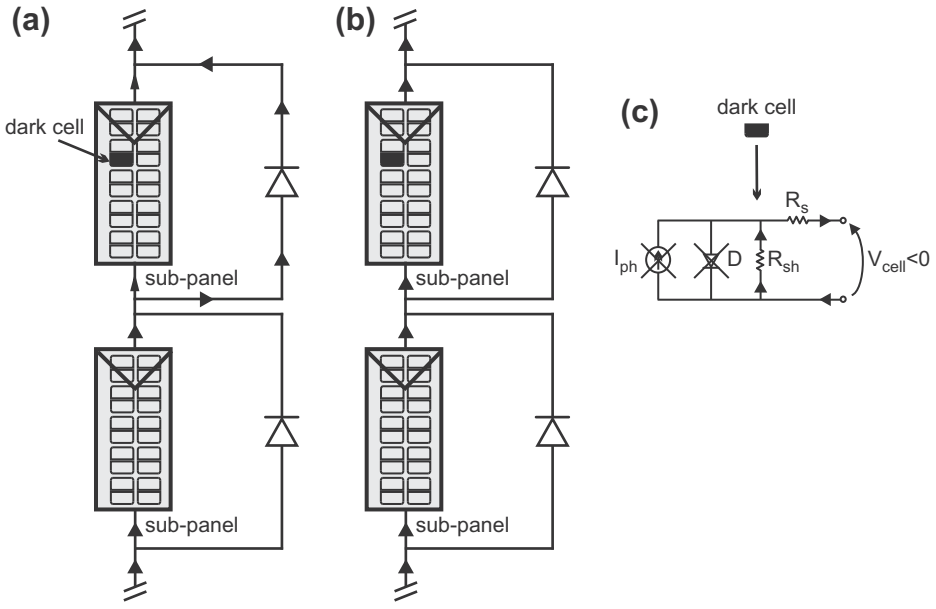

Fig. 3. Schematic representation of the PV panel (partitioned into two 20-cell sub-panels) including the cell intentionally kept under ideally dark conditions: (a) current flow for the V_{string} range wherein the diode is enabled to conduct the bypass current, (b) current flow corresponding to the quasi-linear $I_{string} - V_{string}$ behavior, and (c) circuit representation of the dark cell, within which the sub-panel current is forced to flow through the shunt and series resistances.

ing the dark cell becomes negative, thereby enabling the bypass diode to support the conduction of the portion of the current imposed by the illuminated cells (I_{ph} = 3 A) that can no longer flow through the sub-panel (=2.58 A, as can be seen in Fig. 4a). The weak sub-panel current (I^* = 0.42 A) is then forced to flow through the shunt resistance of the dark cell. Such a scenario is schematically depicted in Fig. 3a. During the bypass phase, the negative sub-panel voltage drop (≈−0.6 V due to the diode activation, as shown in Fig. 4b) unevenly distributes across the 20 cells: in particular, the dark cell is subject to a high *negative* voltage (≈−12.5 V) that allows the conduction of the sub-panel current via shunt resistance (Fig. 3c); instead, the other 19 sunny cells in the sub-panel share a *positive* drop (≈0.63 V) needed to activate the inherent (i.e., parasitic) cell diodes, which must counteract the photocurrent in order to reduce the current of the cells to the level imposed by the shading (i.e., by the dark cell). For string voltages higher than 20 V, also the cell diodes of the illuminated modules start conducting, and the string current I_{string} decreases; as the voltage reaches 37 V, I_{string} equates the current I^* flowing in the dark cell, and the bypass diode is switched off (Fig. 3b). By further increasing the string voltage, the current almost linearly reduces before annihilating (at V_{string} = V_{oc}) and then becoming negative. The circuit behavior within the voltage span comprised between the bypass deactivation and V_{oc} (also denoted as "quasi-linear" region in the following) can be explained as follows. The increase in V_{string} gives rise to a growth in the voltage drops over

(i) the dark cell, i.e., across the shunt resistance to be extracted, referred to as $R_{sh,dark}$ in this description;
(ii) the total series resistance $R_{s,string}$, given by Eq. (1), where N = 2, M = 40 for the case analyzed;
(iii) the parasitic diodes of all the $N \cdot M - 1$ sunny cells in the string, which must conduct an increasingly higher current.

In particular, the purely resistive contributions (i) and (ii), initially negative, reach 0 V as I_{string} = 0 A (i.e., as V_{string} = V_{oc}). It can be also observed that the voltage drop across the sub-panel including the dark cell becomes positive and increases up to 12.6 V, while those corresponding to the illuminated sub-panels somewhat grow (of about 100 mV) to reduce the drops over the series resistances and enhance the current conduction aptitude of the inherent cell diodes, as illustrated in Fig. 4b.

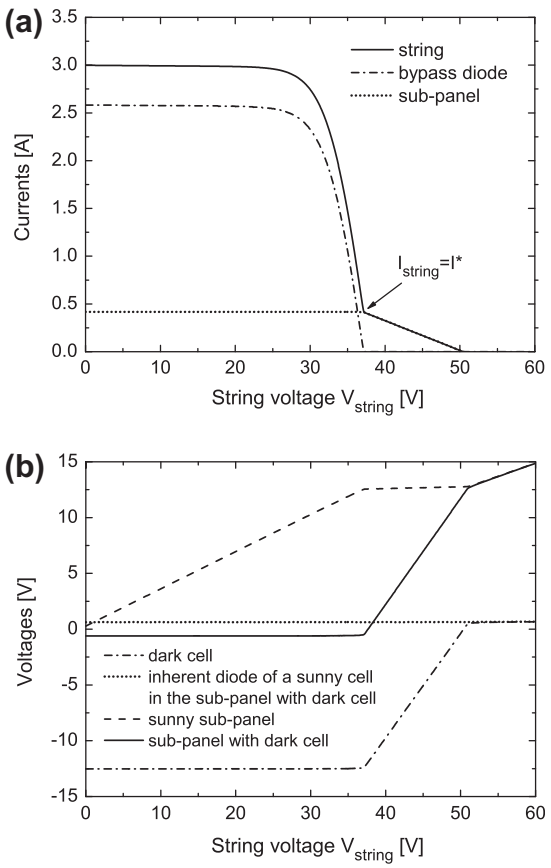

Fig. 4. Evolutions of the key electrical signals, namely, (a) currents and (b) voltages as a function of string voltage, as obtained through calibrated PSPICE simulations by keeping one cell under ideally dark conditions – which is achieved by setting the photocurrent to zero.

The resistance R_{ql}, defined as the absolute value of the reciprocal of the $I_{string} - V_{string}$ slope within the quasi-linear region, can be mathematically expressed as follows:

$$R_{ql} = -\frac{dV_{string}}{dI_{string}} = R_{sh,dark} + R_{s,string} - (N \cdot M - 1) \cdot \frac{dV_{diode}}{dI_{string}} \quad (4)$$

which can be also written in the form:

$$R_{ql} = R_{sh,dark} + R_{s,string} + (N \cdot M - 1) \cdot R_{diode} \quad (5)$$

where $R_{diode} = \frac{dV_{diode}}{dI_{diode}} = -\frac{dV_{diode}}{dI_{string}}$ is the differential resistance associated to the parasitic diode of a sunny cell. The expression of this parameter – which depends on the operating point of the diodes, and therefore on the I_{string} level – can be derived by referring to the single-diode model in Fig. 2, and is given by:

$$R_{diode} = \frac{d}{dI_{diode}}\left[n \cdot V_T \cdot \ln\left(1 + \frac{I_{diode}}{I_0}\right)\right] = \frac{n \cdot V_T}{I_0 + I_{diode}} \approx \frac{n \cdot V_T}{I_{ph} - I_{string}} \approx \frac{n \cdot V_T}{I_{sc} - I_{string}} \quad (6)$$

which evidences that R_{ql} decreases with reducing the string current.

PSPICE simulations were employed to illustrate the impact of the shunt resistance on the current–voltage characteristic of a 2-panel string. All the elementary cells were assumed to share the same R_{sh} value for the sake of simplicity. Fig. 5 shows the $I_{string} - V_{string}$ curves as obtained by fully shading a chosen cell and varying R_{sh} from 10 to 500 Ω. It can be inferred that the curve is almost insensitive to R_{sh} as long as the bypass action is carried out; conversely, incrementing R_{sh} yields a perceptible reduction in the absolute value of the slope in the quasi-linear region, which also slightly shrinks due to the lowered current handling capability of the dark cell, yet remaining wider than 10 V.

If $R_{s,string}$ is determined by resorting to Eq. (2), the shunt resistance of the dark cell $R_{sh,dark}$ can be expressed as:

$$R_{sh,dark} = R_{ql} + \left.\frac{dV_{string}}{dI_{string}}\right|_{V_{string}=V_{oc}} + N \cdot M \cdot \frac{n \cdot V_T}{I_{sc}} - (N \cdot M - 1) \cdot \frac{n \cdot V_T}{I_{sc} - I_{string}} \quad (7)$$

which, being $N \cdot M - 1 \gg 1$, can be reasonably approximated as:

$$R_{sh,dark} \approx R_{ql} + \left.\frac{dV_{string}}{dI_{string}}\right|_{V_{string}=V_{oc}} - N \cdot M \cdot n \cdot V_T \cdot \left(\frac{1}{I_{sc} - I_{string}} - \frac{1}{I_{sc}}\right) \quad (8)$$

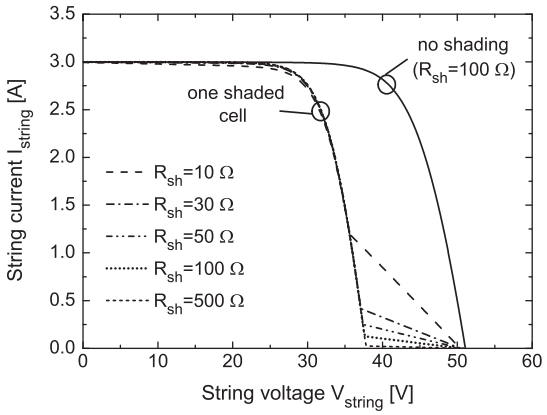

Fig. 5. Simulated $I_{string} - V_{string}$ characteristics of the 2-panel string as obtained by keeping one cell under ideally dark conditions and varying the R_{sh} commonly shared by all cells: (dashed line) $R_{sh} = 10\ \Omega$, (dot-dashed) $R_{sh} = 30\ \Omega$, (dot-dot-dashed) $R_{sh} = 50\ \Omega$, (dotted) $R_{sh} = 100\ \Omega$, and (short-dashed) $R_{sh} = 500\ \Omega$; also shown is (solid line) the curve obtained under full illumination by assuming $R_{sh} = 100\ \Omega$ for all cells.

In a similar fashion, when Eq. (3) is employed, $R_{sh,dark}$ is given by:

$$R_{sh,dark} \approx R_{ql} - 2\frac{V_{oc}}{I_{sc}} + 2\frac{P_A}{I_{sc}^2} + N \cdot M \cdot n \cdot V_T \cdot \left(\frac{2}{I_{sc}} - \frac{1}{I_{sc} - I_{string}}\right) \quad (9)$$

Hence, the shunt resistance of the intentionally-obscured cell $R_{sh,dark}$ can be determined by (i) evaluating a resistance R_{qlm} from the slope of the straight line that guarantees the best fit with the measured $I_{string} - V_{string}$ behavior within the whole quasi-linear region (R_{qlm} can be interpreted as the medium value of the current-dependent resistance R_{ql}) and subsequently (ii) adopting one of the following expressions derived from Eqs. (8) and (9), respectively:

$$R_{sh,dark} \approx R_{qlm} + \left.\frac{dV_{string}}{dI_{string}}\right|_{V_{string}=V_{oc}} - N \cdot M \cdot n \cdot V_T \cdot \left(\frac{1}{I_{sc} - I^*/2} - \frac{1}{I_{sc}}\right) \quad (10)$$

$$R_{sh,dark} \approx R_{qlm} - 2\frac{V_{oc}}{I_{sc}} + 2\frac{P_A}{I_{sc}^2} + N \cdot M \cdot n \cdot V_T \cdot \left(\frac{2}{I_{sc}} - \frac{1}{I_{sc} - I^*/2}\right) \quad (11)$$

where $I^*/2$ represents the average value of I_{string} in the quasi-linear region (I^* is known from the measurement), and is usually a small fraction of the short-circuit current I_{sc} unless the selected cell exhibits a very low $R_{sh,dark}$.

The following remarks can be made:

- The proposed approach is non-intrusive, i.e., it does not require the de-encapsulation and removal of the selected cell from the module.
- The extraction of R_{qlm} is not prone to errors due to the wide voltage range within which the quasi-linear behavior arises (>10 V regardless of the number of panels connected in series); conversely, the useful voltage range may shrink to less than 0.5 V when determining R_{sh} from the *I–V* characteristic of a single cell, especially in the presence of soft breakdown [6], [25], [26].
- The ideality factor n, included in the equivalent cell model to describe the effect of recombination of electron–hole pairs in the space–charge region, is generally unknown, which generates an uncertainty on the $R_{sh,dark}$ evaluation by using Eqs. (10) and (11); moreover, this error is proportional to the number of cells connected in the string $N \cdot M$. In principle one might tackle this problem by adopting Eq. (8) and extracting R_{ql} from the slope of a restricted portion of the quasi-linear $I_{string} - V_{string}$ curve around $V_{string} = V_{oc}$, thus reducing the n-dependent term; however, this would exclude the aforementioned advantage of the proposed approach, i.e., the possibility of determining a slope in a wide V_{string} range.

In order to understand whether Eqs. (10) and (11) can be successfully employed without accurately knowing the value of the ideality factor n of the inherent diodes, we resorted to the following procedure. Two PV strings with $N = 2$ and $N = 10$ (both with $M = 40$) were built in PSPICE to apply the above techniques to the *simulated I–V* curves corresponding to $I_{ph} = 3$ A. As a result, the extracted $R_{sh,dark}$ value can be compared with the *known* shunt resistance of the selected cell, thereby allowing an estimation of the reliability of the methods. In particular, the value 1.3 was assumed for n in Eqs. (10) and (11). The analysis was carried out by varying in PSPICE the "actual" *unknown* ideality factor n in the range 1–1.6; higher values were not considered since R_{qlm} is to be extracted in a region within which the conduction of sunny diodes should in principle be dominated by diffusion [39]. The comparison between

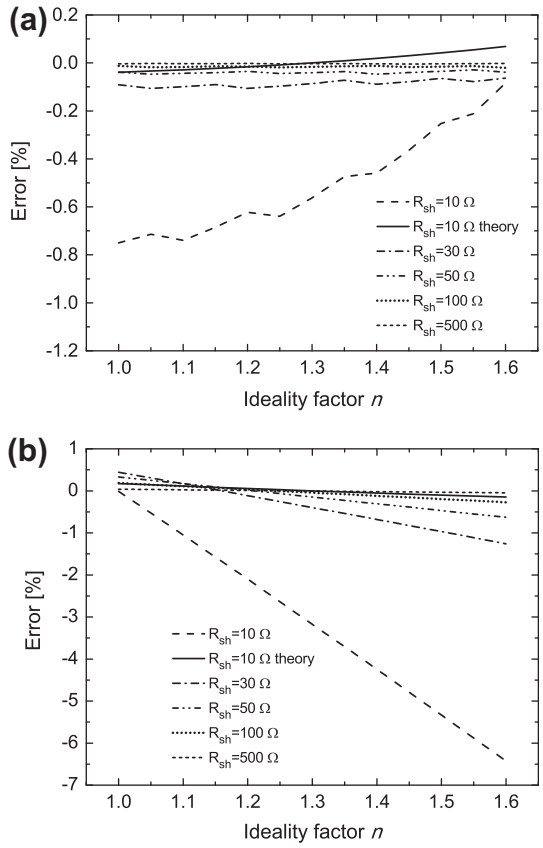

Fig. 6. Percentage error as a function of ideality factor for a 2-panel string by using (a) Eq. (10) and (b) Eq. (11) for various R_{sh} values: (dashed line) $R_{sh} = 10\ \Omega$, (dot-dashed) $R_{sh} = 30\ \Omega$, (dot-dot-dashed) $R_{sh} = 50\ \Omega$, (dotted) $R_{sh} = 100\ \Omega$, and (short-dashed) $R_{sh} = 500\ \Omega$; also shown are (solid lines) the theoretical n-induced errors as determined from (a) Eq. (12) and (b) Eq. (13), respectively.

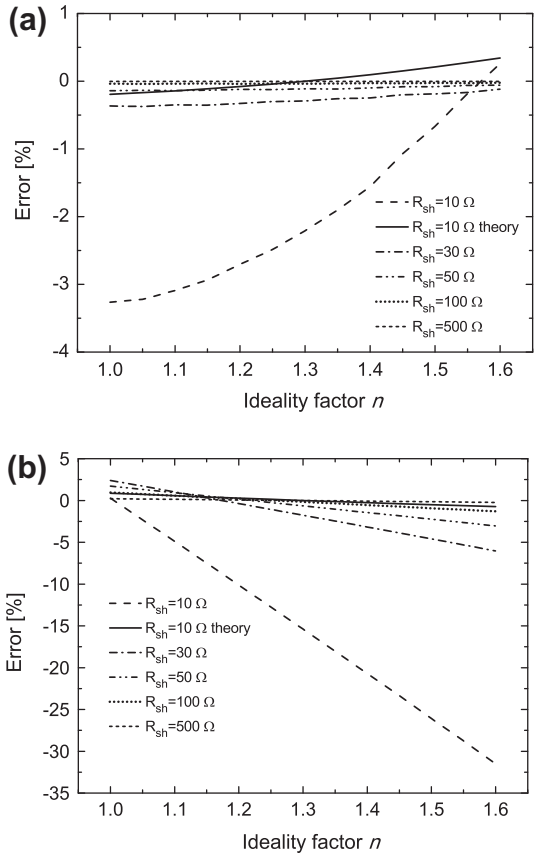

Fig. 7. Percentage error as a function of ideality factor for a 10-panel string by employing (a) Eq. (10) and (b) Eq. (11) for various R_{sh} values: (dashed line) $R_{sh} = 10\ \Omega$, (dot-dashed) $R_{sh} = 30\ \Omega$, (dot-dot-dashed) $R_{sh} = 50\ \Omega$, (dotted) $R_{sh} = 100\ \Omega$, and (short-dashed) $R_{sh} = 500\ \Omega$; also shown are (solid lines) the theoretical n-induced errors as determined from (a) Eq. (12) and (b) Eq. (13), respectively.

the extracted and real $R_{sh,dark}$ as a function of n was performed for various values of R_{sh} commonly assigned to all the shunt resistances of the cells in the PSPICE string (including the $R_{sh,dark}$ to be measured), namely, 10, 30, 50, 100, and 500 Ω.[1] The percentage errors corresponding to the 2-panel string are reported in Fig. 6a and b for Eqs. (10) and (11), respectively. As far as Eq. (10) is concerned, it is found that, regardless of R_{sh} and n, the error is always negative and lower than 0.8% (for $R_{sh} > 20\ \Omega$ it does not exceed 0.2%), that is, an excellent degree of accuracy is achieved. It is worth noting that the theoretical absolute error solely due to n, given by:

$$R_{sh,dark}(\text{extracted}) - R_{sh,dark}(\text{real}) = -N \cdot M \cdot (1.3 - n) \cdot V_T \cdot \left(\frac{1}{I_{sc} - I^*/2} - \frac{1}{I_{sc}}\right) \quad (12)$$

should be negative for $n < 1.3$, positive for $n > 1.3$, and lower – in absolute value – than that obtained through the proposed approach. This can be inferred by observing the curve obtained from Eq. (12) in Fig. 6a for the case in which all R_{sh} are equal to 10 Ω. This discrepancy can be explained by noting that Eq. (2) – on which Eq. (10) is based – is derived by disregarding the shunt current for all cells in the string (i.e., $R_{sh} \to \infty$), which entails an increasing underestimation of $R_{sh,dark}$ as the value of the shunt resistance common to all cells is reduced. A lower accuracy is obtained by adopting Eq. (11) with $n = 1.3$; in particular, the error is lower than 1% as long as the shunt resistance is larger than 30 Ω, while rapidly growing to almost 7% as $R_{sh} = 10\ \Omega$ and $n = 1.6$. It is to be remarked that also in this case a discrepancy occurs with respect to the error due to the mere uncertainty on the ideality factor, which, according to:

$$R_{sh,dark}(\text{extracted}) - R_{sh,dark}(\text{real}) = N \cdot M \cdot (1.3 - n) \cdot V_T \cdot \left(\frac{2}{I_{sc}} - \frac{1}{I_{sc} - I^*/2}\right) \quad (13)$$

should be positive for $n < 1.3$ and negative for $n > 1.3$, independently of R_{sh}. This is due to the fact that – similarly to Eq. (2) – also Eq. (3) suffers from the assumption of $R_{sh} \to \infty$, i.e., it is rigorously valid only if shunt paths are absent for all the cells connected in the string. In particular, Eq. (3) is much more affected by this approximation than Eq. (2) due to the significant sensitivity of $R_{s,string}$ to even small R_{sh}-induced variations of the area beneath the illuminated $I_{string} - V_{string}$ curve. PSPICE simulations allowed indeed demonstrating that, if the cells exhibit low shunt resistance, Eq. (3) may provide markedly inaccurate $R_{s,string}$ values even though the ideality factor n is assumed to be known:[2] if $n = 1.3$ and $R_{sh} = 10\ \Omega$ are chosen for all cells in the 2-panel array, errors amounting to 1.5% and 25% are indeed achieved when evaluating $R_{s,string}$ from Eqs. (2) and (3), respectively, with $n = 1.3$. This in turn reduces the accuracy of Eq. (11) compared to Eq. (10), as can be evinced from Fig. 6a and b. The reliability of the extraction methods

[1] For the sake of simplicity, the PSPICE simulations were carried out by assuming all cells ideally identical and subject to the same irradiation, except for the intentionally obscured cell, the photocurrent I_{ph} of which was set to 0 A.

[2] The inaccuracy of the *area method* [38] applied to an individual cell due to the assumption of negligible shunt loss at low illumination was already noted in [40].

worsens by incrementing the number of cells in the string, as illustrated in Fig. 7, which reports the errors corresponding to a 10-panel array by applying Eq. (10) (Fig. 7a) and Eq. (11) (Fig. 7b). This is due to a twofold reason: (i) the assumption of absence of shunt loss in Eqs. (2) and (3) plays an increasingly relevant role as $N \cdot M$ grows, and – to a smaller extent – and (ii) the errors due to the n indetermination described by Eqs. (12) and (13), shown in Fig. 7 for the case of $R_{sh} = 10\ \Omega$ shared by all the cells in the string, are directly proportional to $N \cdot M$. Nevertheless, Fig. 7a clarifies that an error lower than 3.5% is encountered when employing Eq. (10), even if all the cells in the string are of very low quality ($R_{sh} = 10\ \Omega$) and the discrepancy between the chosen and the real ideality factor is as high as 0.3. By converse, errors higher than 30% can be found as Eq. (11) is adopted, mainly due to the significant inaccuracy of the generalized *area method* induced by the $R_{sh} \to \infty$ assumption.

As a rule of thumb, one can safely adopt Eq. (10) by considering an ideality factor value ranging e.g., between 1.2 and 1.4, for monocrystalline silicon strings whose product $N \cdot M$ is lower than 500, which covers most residential PV systems; this allows indeed confining the maximum achievable error within reasonable bounds even if the elementary cells share very low R_{sh} values.

4. Experimental results and discussion

The proposed method was applied to the 10-panel string described in Section 2. As a first step, some $I_{string} - V_{string}$ characteristics were measured at sunny midday in the absence of shading. The series resistance $R_{s,string}$ was then evaluated by adopting the two string-oriented approaches introduced in Section 3. However, a significant difference between the corresponding results was obtained: $R_{s,string}$ was found to lie in the ranges 5.13 Ω–5.30 Ω and 7.50 Ω–9.20 Ω by applying Eqs. (2) and (3), respectively, to all the experimental curves. This discrepancy was ascribed to an intrinsic error-sensitivity of Eq. (3) in determining the series resistance of a string comprising a high number of panels, which can be explained as follows: even in presence of full sunlight, the area P_A under the $I_{string} - V_{string}$ curve is somewhat lower than that corresponding to an ideal mismatch-free string, due to the manufacturing tolerance and the slightly uneven irradiation over the modules; unfortunately, a small P_A deviation with respect to the ideal case turns into a significant error in the evaluation of $R_{s,string}$.[3] This is another reason to prefer Eq. (2) to Eq. (3), which was not evidenced in Section 3 since the PSPICE-based analysis was carried out by assuming all the cells ideally identical. Further evidence of the proneness to error of the extended *area method* was provided through simulations of the 10-panel string performed by intentionally inducing small differences among the cells in terms of irradiation and parameters of diode/resistances. From the more reliable results attained through Eq. (2), the average series resistance R_s of the individual cells was determined to be about 13 mΩ. The parameters I_{sc} and $\left.\frac{dV_{string}}{dI_{string}}\right|_{V_{string}=V_{oc}}$ needed for the application of Eq. (10) were also available.

Afterward, a prescribed cell was obscured with an opaque tape and the current–voltage curve of the string was measured in order to extract R_{qlm} from the quasi-linear region; $R_{sh,dark}$ was then evaluated from Eq. (10) by assuming the ideality factor n equal to 1.2. The procedure was then repeated for a large number of cells so as to achieve an exhaustive map of R_{sh} values over the whole string. The experimental quasi-linear regions corresponding to a few cases are reported in Fig. 8; it must be noted that the slopes are considerably different, although virtually identical PV modules are connected in series. Fig. 9 illustrates the R_{sh} values extracted for two cells per panel. The results of this investigation can be summarized as follows: (i) the shunt resistances fall in a surprisingly wide range spanning from 30 to 300 Ω, which implies that the specific resistance spreads from 2 to 20 kΩ cm^2; (ii) thus, the average cell quality is relatively low, since values larger than 400/500 Ω are expected in good silicon PV cells [3,4,41]; (iii) over a prescribed module, the cells show a quite uniform R_{sh} distribution; (iv) the measurements were repeated under different irradiation intensities leading to a short-circuit current I_{sc} spanning from 2.0 to 2.5 A, and the extracted R_{sh} values were found to be almost constant, consistently with the conclusion reached in [23].

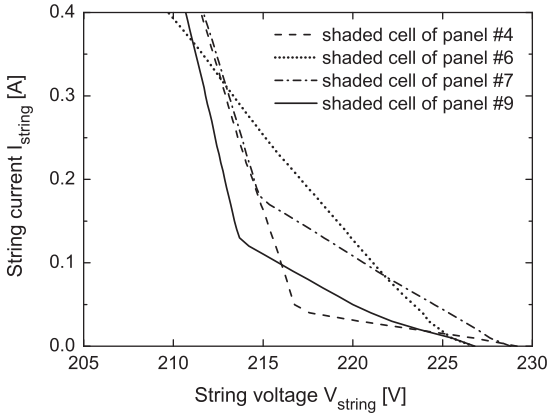

Fig. 8. Experimental $I_{string} - V_{string}$ characteristics as obtained by intentionally shading assigned individual cells. The curves are measured under slightly different irradiation levels.

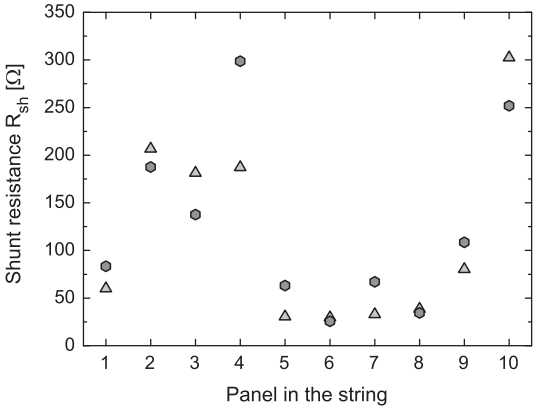

Fig. 9. Experimentally extracted shunt resistance values for the 10 panels composing the string; for each panel, two cells were measured.

5. Conclusion

In this work, a simple non-intrusive approach to accurately assess the shunt resistance of a chosen PV cell embedded in an installed string is proposed, which does not require preliminary evaluation of the parameters associated to the intrinsic diodes. The technique relies on the measurement of the current–voltage characteristic of the whole string while intentionally keeping the selected cell under ideally dark conditions. The shunt resistance is then determined from the slope of the curve in the voltage range where the string exhibits a quasi-resistive behavior; in particular,

[3] As an example, the area P_A beneath an experimental $I_{string} - V_{string}$ characteristic was determined to be equal to 465.6 W for a short-circuit current $I_{sc} = 2.25$ A so that the term $2\frac{P_A}{I_{sc}^2}$ in Eq. (3) amounts to about 184 Ω. Consequently, a P_A reduction of 1.5% due to a slight mismatch reflects into an increase of 3 Ω in the extracted $R_{s,string}$.

the slope extraction is not critical since such a range can be 10–15 V wide, regardless of the number of panels connected in series.

An extensive simulation-based analysis has allowed proving that the approach can be successfully applied even to strings comprising hundreds of low-quality cells, if the extended *method of the slope at the V_{oc} point* is used to evaluate the total series resistance of the array.

The proposed method has been adopted to evaluate the shunt resistance of prescribed cells of a PV array composed by 10 commercial silicon modules; the estimated specific resistances are found to span from 2 to 20 $k\Omega\,cm^2$, while being almost uniform over a given panel. It can be therefore concluded that the impact of defects can be considerably different even for panels belonging to the same family.

The procedure can be exploited for undemanding performance characterization, quality testing, and failure analysis of the module at a cell level; in particular, the degrading effect of the prolonged exposure to light can be monitored over long times.

Acknowledgment

This work was financially supported by ISET Energia S.r.l., Valle di Maddaloni, Italy.

References

[1] Green MA. Solar cells: operating principles, technology and system applications. The University of New South Wales; 1986.
[2] Stirn RJ. Junction characteristics of silicon solar cells. In: Proceedings of IEEE photovoltaic specialists conference (PVSC) 1972:72–82.
[3] Lucheng Z, Hui S. Novel approach for characterizing the specific shunt resistance caused by the penetration of the front contact through the P–N junction in solar cell. J Semicond 2009;30(7):0740071–73.
[4] Priyanka, Lal M, Singh SN. Effect of localized inhomogeneity of shunt resistance on the spectral response and dark I–V characteristics of silicon solar cell. In: Proceedings of IEEE photovoltaic energy conference 2006:1242–4.
[5] McMahon TJ, Basso TS, Rummel SR. Cell shunt resistance and photovoltaic module performance. In: Proceedings of IEEE photovoltaic specialists conference (PVSC) 1996:1291–4.
[6] van Dyk EE, Meyer EL. Analysis of the effect of parasitic resistances on the performance of photovoltaic modules. Renewable Energy 2004;29(3):333–44.
[7] Meyer EL, van Dyk EE. The effect of reduced shunt resistance and shading on photovoltaic module performance. In: Proceedings of IEEE photovoltaic specialists conference (PVSC) 2005:1331–4.
[8] Banerjee S, Anderson WA. Temperature dependence of shunt resistance in photovoltaic devices. Appl Phys Lett 1986;49(1):38–40.
[9] Salinger J. Measurement of solar cell parameters with dark forward *I–V* characteristics. Acta Polytechnica 2006;46(4):25–7.
[10] Phang JCH, Chan DSH, Phillips JR. Accurate analytical method for the extraction of solar cell model parameters. Electron Lett 1984;20(10):406–8.
[11] Polman A, Van Sark WGJHM, Sinke W, Saris FW. A new method for the evaluation of solar cell parameters. Solar Cells 1986;17(2/3):241–51.
[12] Chan DSH, Phillips JR, Phang JCH. A comparative study of extraction methods for solar cell model parameters. Solid-State Electron 1986;29(3):329–37.
[13] Chegaar M, Ouennoughi Z, Guechi F. Extracting dc parameters of solar cells under illumination. Vacuum 2004;75(4):367–72.
[14] Celik AN, Acikgoz N. Modelling and experimental verification of the operating current of mono-crystalline photovoltaic modules using four- and five-parameter models. Appl Energy 2007;84(1):1–15.
[15] Ishibashi K, Kimura Y, Niwano M. An extensively valid and stable method for derivation of all parameters of a solar cell from a single current–voltage characteristic. J Appl Phys 2008;103:094507-1–7-6.
[16] Khan F, Singh SN, Husain M. Effect of illumination intensity on cell parameters of a silicon solar cell. Solar Energy Mater Solar Cells 2010;94(9):1473–6.
[17] Kennerud KL. Analysis of performance degradation in CdS solar cells. IEEE Trans Aerospace Electron Syst 1969;AES-5(6):912–7.
[18] Charles JP, Abdelkrim M, Muoy YH, Mialhe P. A practical method of analysis of the current–voltage characteristics of solar cells. Solar Cells 1981;4(2):169–78.
[19] Gow JA, Manning CD. Development of a photovoltaic array model for use in power-electronics simulation studies. IEE Proc Electric Power Appl 1999;146(2):193–200.
[20] Kaminski A, Marchand JJ, Laugier A. Non ideal dark *I–V* curves behavior of silicon solar cells. Solar Energy Mater Solar Cells 1998;51(3/4):221–31.
[21] Wolf M, Rauschenbach H. Series resistance effects on solar cell measurements. Adv Energy Convers 1963;3:455–79.
[22] Fuchs D, Sigmund H. Analysis of the current–voltage characteristic of solar cells. Solid-State Electron 1986;29(8):791–5.
[23] Priyanka, Lal M, Singh SN. A new method of determination of series and shunt resistances of silicon solar cells. Solar Energy Mater Solar Cells 2007;91(2/3):137–42.
[24] Dallago E, Finarelli D, Merhej P. Method based on single variable to evaluate all parameters of solar cells. Electron Lett 2010;46(14):1022–4.
[25] Lal R, Sharan R. Shunt resistance and soft reverse characteristics of silicon diffused-junction solar cells. Solid-State Electron 1986;29(10):1015–23.
[26] Schroder DK. Semiconductor material and device characterization. John Wiley and Sons, Inc.; 1990.
[27] El-Adawi MK, Al-Nuaim IA. A method to determine the solar cell series resistance from a single *I–V* characteristic curve considering its shunt resistance – new approach. Vacuum 2002;64(1):33–6.
[28] Datta SK, Mukhopadhyay K, Bandopadhyay S, Saha H. An improved technique for the determination of solar cell parameters. Solid-State Electron 1992;35(11):1667–73.
[29] Bouzidi K, Chegaar M, Bouhemadou A. Solar cell parameters evaluation considering the series and shunt resistance. Solar Energy Mater Solar Cells 2007;91(18):1647–51.
[30] Jervase JA, Bourdoucen H, Al-Lawati A. Solar cell parameter extraction using genetic algorithms. Meas Sci Technol 2001;12(11):1922–5.
[31] Chan DSH, Phang JCH. A method for the direct measurement of solar cell shunt resistance. IEEE Trans Electron Dev 1984;ED-31(3):381–3.
[32] OrCAD PSPICE 9.1 Reference Guide, OrCAD, Inc., 1999.
[33] Gargiulo M, Guerriero P, Daliento S, Irace A, d'Alessandro V, Crisci M, et al. A novel wireless self-powered microcontroller-based monitoring circuit for photovoltaic panels in grid-connected systems. In: Proceedings IEEE international symposium on power electronics, electrical drives, automation and motion (SPEEDAM); 2010. p. 164–8.
[34] Datasheet available at www.hoecherl-hackl.com.
[35] Ramaprabha R, Mathur BL. Impact of partial shading on solar PV module containing series connected cells. Int J Recent Trends Eng 2009;2(7):56–60.
[36] Tarr NG, Pulfrey DL. The superposition principle for homojunction solar cells. IEEE Trans Electron Dev 1980;ED-27(4):771–6.
[37] Bashahu H, Habyarimana A. Review and test of methods for determination of the solar cell series resistance. Renew Energy 1995;6(2):129–38.
[38] Araujo GL, Sánchez E. A new method for experimental determination of the series resistance of a solar cell. IEEE Trans Electron Dev 1982;ED-29(10):1511–3.
[39] Jia Q, Anderson WA, Liu E, Zhang S. A novel approach for evaluating the series resistance of solar cells. Solar Cells 1988;25(3):311–8.
[40] Phang JCH, Chan DSH, Wong YK. Comments on the experimental determination of series resistance in solar cells. IEEE Trans Electron Dev 1984;ED-31(5):717–8.
[41] Sharma SK, Samuel KB, Srinivasamurthy N, Agrawal BL. Overcoming the problems in determination of solar cell series resistance and diode factor. J Phys D: Appl Phys 1990;23(9):1256–60.